remote sensing

MDPI

Article

Spatial-Temporal Evaluation of Satellite-Derived Rainfall Estimations for Water Resource Applications in the Upper Congo River Basin

Alaba Boluwade

School of Climate Change & Adaptation, University of Prince Edward Island, Charlottetown, PE C1A 4P3, Canada; aboluwade@upei.ca

Abstract: Satellite rainfall estimates are robust alternatives to gauge precipitation, especially in Africa, where several watersheds and regional water basins are poorly gauged or ungauged. In this study, six satellite precipitation products, the Climate Hazards Group Infrared Precipitation with Stations (CHIRPS); Tropical Applications of Meteorology Using Satellite and Ground-based Observations (TAMSAT); TRMM Multi-satellite Precipitation Analysis (TMPA); and the National Aeronautics and Space Administration's new Integrated Multi-SatellitE Retrievals for Global Precipitation Measurement (GPM) early run (IMERG-ER), late run (IMERG-LR), and final run (IMERG-FR), were used to force a gauge-calibrated Soil & Water Assessment Tool (SWAT) model for the Congo River Basin, Central Africa. In this study, the National Centers for Environmental Prediction's Climate Forecast System Reanalysis (CFSR) calibrated version of the SWAT was used as the benchmark/reference, while scenario versions were created as configurations using each satellite product identified above. CFSR was used as an independent sample to prevent bias toward any of the satellite products. The calibrated CFSR model captured and reproduced the hydrology (timing, peak flow, and seasonality) of this basin using the average monthly discharge from January 1984–December 1991. Furthermore, the results show that TMPA, IMERG-FR, and CHIRPS captured the peak flows and correctly reproduced the seasonality and timing of the monthly discharges (January 2007–December 2010). In contrast, TAMSAT, IMERG-ER, and IMERG-LR overestimated the peak flows. These results show that some of these precipitation products must be bias-corrected before being used for practical applications. The results of this study will be significant in integrated water resource management in the Congo River Basin and other regional river basins in Africa. Most importantly, the results obtained from this study have been hosted in a repository for free access to all interested in hydrology and water resource management in Africa.

Keywords: SWAT; Congo River Basin; surface water; afforestation; water resources management; satellite precipitation; Africa

Citation: Boluwade, A. Spatial-Temporal Evaluation of Satellite-Derived Rainfall Estimations for Water Resource Applications in the Upper Congo River Basin. *Remote Sens.* **2024**, *16*, 3868. https://doi.org/10.3390/rs16203868

Academic Editors: Haonan Chen and Haoran Li

Received: 8 August 2024
Revised: 10 October 2024
Accepted: 10 October 2024
Published: 18 October 2024

1. Introduction

Many of the world's watersheds and river basins are ungauged. This is a significant challenge, especially in water resource management projects dealing with precipitation estimates and distributions. An accurate and reliable precipitation dataset is crucial since this is the foremost and fundamental component of the hydrologic cycle. A lack of accurate and consistent precipitation records is common in Africa, where many watersheds are ungauged or sparsely gauged. In many African watersheds, historical precipitation records of available observed data are filled with missing values. Hydrologic applications need complete, seamless, and consistent datasets to make an informed decision. Using an incomplete and missing dataset can introduce bias and erroneous interpretation. Radar- and satellite-based rainfall estimates have proven to be a good proxy for observed precipitations from weather stations [1,2]. Radar is expensive, and its use is limited, especially for developing nations in sub-Saharan African countries. Therefore, satellite-based rainfall products

that are free and cover large areas, especially for large river basins, will be the right solution. The spatial and temporal resolutions of satellite-based rainfall products are also sufficient for several large river basins in Africa, such as the Congo River Basin (hereafter: CRB) or Niger River Basin. Several of these available satellite products include the Climate Hazards Group Infra-Red Precipitation with Station data (CHIRPS; [3]); Tropical Rainfall Measuring Mission (TRMM) Multi-satellite Precipitation Analysis (TMPA) (TMPA-3B42; [4–6]); Tropical Applications of Meteorology using Satellite and Ground-based Observations (TAMSAT, [7]); and Integrated Multi-satellitE Retrievals for GPM (IMERG; [8]). Others include the Global Precipitation Climatology Centre (GPCC) developed by the World Climate Research Program (WCRP); Precipitation Estimation from Remotely Sensed Information using Artificial Neural Networks-Climate Data Record (PERSIANN-CDR; [9]); Climate Precipitation Center Morphing Technique (CMORPH; [10]); and Africa Rainfall Climatology Version 2 (ARC2; [11]). Several of these products have been used as hydrologic forcing in Africa. Munzimi et al. [12] used TMPA (3B43_V6) to quantify the rainfall pattern over the entire CRB. The authors reported that these satellite data performed well in the basin. Further, Nicholson et al. [13] evaluated nine satellite-based rainfall products over the CRB. These satellite products include CHIRPS (version 2), GPCP (2.3), TMPA (3B43), and PERSIANN-CDR. Other studies that have quantified the performance of various satellite products over the CRB include [14–17]. Datok et al. [18] investigated Cuvette Centrale's role in CRB's hydrology. In their study, the authors concluded that runoff from the Congo River headwater was the largest contributor to this peatland. Kitambo et al. [19] also applied in situ and satellite-derived observations to quantify the surface hydrology of CRB. They reported that northern sub-basins and central regions make the largest contributions to the large peak flow in December–January. In contrast, the southern basins supply water to the peak flows in April–May. This study does not aim to provide a review but rather to quantify the reliability of the chosen satellite products in the CRB.

Africa has more than 52 major river basins, which provide ecosystem service benefits for more than 150 million people. The CRB is the largest river basin in Africa, with more than 3 million km^2 in land area. The CRB is the second largest carbon deposit/sink (after the Amazon River Basin) in the world [20]. The CRB is also one of the world's greatest sources of hydroelectric potential. According to the World Bank, the CRB's hydropower potential is estimated to have the capacity to light up the entire African continent [20]. In addition, the CRB is important for the water resource management, food provision, and source of livelihood for more than 75 million people in Africa [21]. The Ubangi River, which drains the northern basins as a whole, is a major tributary of the Congo River. In addition, this river forms the administrative boundary between the CAR and the DRC. The northern sub-basins (Ubangi and Quesso basins) have been affected by a reduction in flow over several decades [22]. This is important because this river is central to and useful for navigation and a source of economic opportunity for the vulnerable population living in this area.

One of the widely applied hydrologic models that can be used to assess the performance of these satellite products is the Soil & Water Assessment Tool (SWAT). This model was developed by [23] and has been applied in various applications and studies. Schuol et al. [24] applied SWAT to predict the hydrologic processes of the entire African continent's basins. The authors quantified the freshwater components such as the water yield, aquifer recharge, actual ET, and soil water. The authors concluded that the products based on satellite only (without gauged adjusted observations) overestimated the peak flows during the rainy season. In addition, other products that are already calibrated with gauge precipitation agree more with the referenced product (TMPA 3B42_V7). There is a possibility of bias in doing this, especially for all satellite products that share similar backgrounds and algorithms with this reference model. The SWAT model needs calibration with the gauged discharge from hydrometric stations. The African Database of Hydrometric Indices (ADHI) was created to provide hydrometric indices for many rivers in Africa. The database has 1466 hydrometric stations with at least 10 years of daily discharge covering 1950 to 2018.

The National Centers for Environmental Prediction's Climate Forecast System Reanalysis (CFSR) climate data, which are from satellite-based rainfall datasets, have special advantages from both spatial and temporal resolution standpoints. Tomy and Suman [25] reported that CFSR is adequate in and reliable as a proxy for gauged precipitation in data-deficient areas. In another study performed using CFSR as hydrologic forcing for an Arctic watershed, Bui and Nie [26] also concluded that this dataset is reliable and can act as a proxy for ground-gauged precipitation. Therefore, this dataset will be used in this study as an independent source of data to calibrate the SWAT model. Tshimanga [27] reviewed the modeling and predictions performed in the CRB. The author argued that over the past two decades, all modeling efforts have only focused on testing modeling performance or experimenting with new models in this data-scarce basin. Several of these studies, however, did not address the real problems or challenges facing the basin. The author further advocated that modeling should support policy- and decision-making that will aid the strategic management of water resources and adaptation to climate change. Therefore, instead of solely conducting a performance evaluation study, the current study went a step further by considering a major climate extreme in the basin and how reliable satellite-based estimations are in capturing or reproducing these events. In addition, the results from this study are shared through an online platform where users can download the data used in this study. Therefore, this study provides a tool for those in this developing and data-scarce region who need information to make water resource management decisions.

It is therefore imperative that the reliability of satellite-based rainfall datasets be evaluated as forcing for hydrologic modeling applications. Therefore, the primary purpose of this paper is to quantify the uncertainty in these satellite products by using them as hydrologic forcing in a hydrologic model. The knowledge about their reliability and usefulness will guide their application in large basins such as the CRB and other African regional watersheds. Given the scarcity of gauge data in Africa and the limited research in this area, the availability of satellite data with continuous observations in both temporal and spatial dimensions holds great potential for applications in Africa. In this regard, this study provides valuable insights and contributes to the existing knowledge in this field.

2. Materials and Methods

2.1. Study Area: Congo River Basin

The CRB (Figure 1) is located between 0°00′N and 25°00′E. It is the second largest river basin in the world and the largest river in Africa, with a drainage area covering 3.4 million km^2. The CRB is shared by nine countries in Africa (Congo Democratic Rep. Central African Angola, Congo Rep. Zambia, Tanzania, Cameroon, Burundi, Rwanda, Gabon, and Malawi). According to Tshimanga et al. [27], the "vegetation cover varies from open savannah grassland and woodland in the upland areas to tropical rainforest in the central basin". Moreover, Lambert et al. [28] also reported that the center of the CRB is dominated by forest land cover, which is approximately 50% of the total area. Further, savannah grasslands comprise over 35% of the total area, with croplands integrated within the natural vegetation [29]. There have recently been increased anthropogenic activities in this area as well. Deforestation and mining activities have also been reported to have an increased trend [30]. The CRB is composed of sandy and clayey soil types. Clay soil dominates both the northern and central sections of the basin [29]. For geologic formations, unconsolidated Cenozoic sediments dominate the central portion of the CRB, and the main catchments that feed this central basin are also dominated by weathered Mesozoic and Precambrian rocks [27,31]. Furthermore, it has been reported that soil type and geologic formations contributed to the variability in the water level in the second half of the last century [32]. Annual precipitation in this basin is over 1500 mm [33]. The mean annual temperature is around 20 °C. Furthermore, because of its close proximity to the equator, it has heterogeneous climatic regimes, with the northern and southern regions experiencing dry and wet seasons, respectively. Moreover, the equatorial area has a bimodal annual precipitation distribution [33]. According to Runge [31], there are seasonal height variations

that are attenuated. There are more than seven sub-basins inside the CRB [34]. At the upper portion of the CRB, the Ubangi River Basin (URB) and Sangha River Basin (SRB) have a drainage area of approximately 645,100 km^2 and 283,400 km^2, respectively. For this study, we combine both river basins (URB and SRB) and represent them as the Upper Congo River Basin (hereafter: UCRB, Figure 1). The Ubangi River is one of the most important tributaries in the UCRB [35].

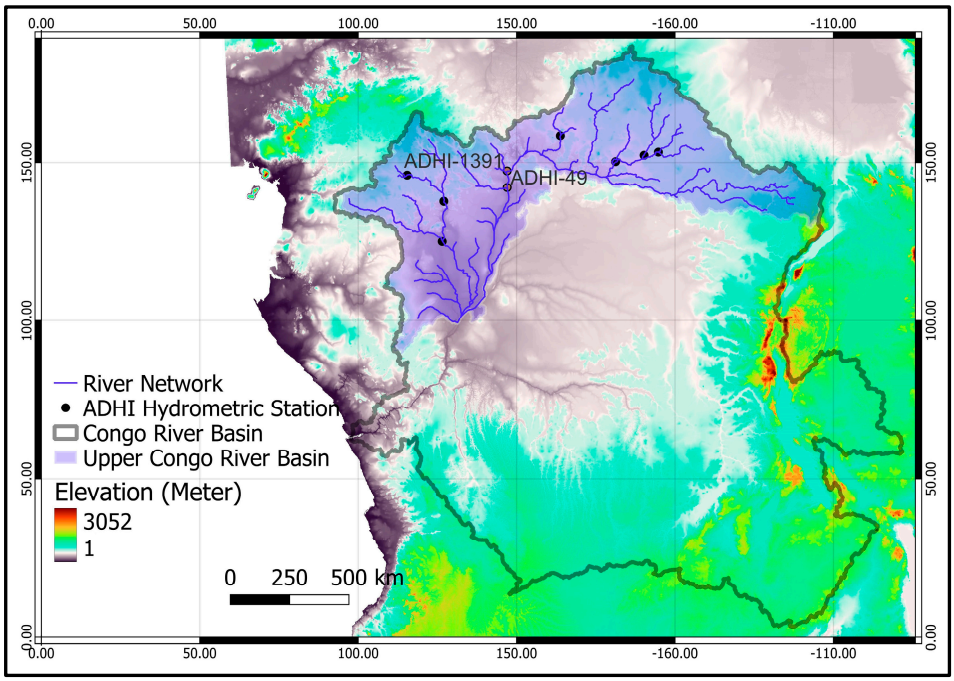

Figure 1. Elevation map of the study area that shows the location of ADHI hydrometric stations (outlets) and the Upper Congo River Basin.

2.2. Description of Datasets

The datasets used for this study will be divided into three categories:

(1) SWAT Inputs: Digital Elevation Model (DEM), Soil and Land Use Maps

The DEM at 30 m resolution was obtained from the United States Geologic Survey (USGS). The land-use datasets were obtained from the European Space Agency (ESA) Climate Change Initiative (CCI) generated in 2015 (https://climate.esa.int/en/projects/land-cover/data/#mrlc-maps-series-from-1992-onwards-(v207-and-v2.1.1), accessed on 5 December 2022). The ESA-CCI is at 300 m resolution. Soil data were obtained from the SWAT Global Data (https://swat.tamu.edu/data/, accessed on 5 December 2022).

(2) Precipitation and Temperature Forcing

The National Centers for Environmental Prediction's CFSR climate data include a satellite-based rainfall dataset. This dataset was obtained from the SWAT global data repository (https://swat.tamu.edu/data/cfsr, accessed on 5 December 2022). Daily precipitation and temperature were extracted from this database. Dile and Srinivasan [36] used this dataset for the Blue Nile River Basin (BNRB), and they concluded that the CFSR was satisfactory in simulating the hydrology of the basin. In addition, Fuka et al. [37] also concluded that using CFSR temperature and precipitation data is as good as gauged observations from weather stations. Therefore, in this paper, both precipitation and temperature will be used to force the reference model, which will be calibrated and used as a benchmark for all other satellite-based rainfall products. This dataset will act as an independent sample for all the satellite-based datasets.

(a) TMPA

The Tropical Rainfall Measuring (TRMM) Multi-satellite Precipitation Analysis (TMPA) research product (TMPA Precipitation L3 1 day 0.25° × 0.25° V7 3B42_Daily; hereafter: TMPA) is the daily accumulated precipitation produced from the 3 hr TRMM multi-satellite precipitation analysis TMPA (3B42). According to Huffman et al. [38], this daily accumulation is obtained by "summing valid retrievals in a grid cell for the data day". This version of the TMPA is already gauge adjusted with selected stations from the weather network. This daily TMPA was downloaded from the National Aeronautics and Space Administration (NASA) Giovanni website (https://disc.gsfc.nasa.gov/datasets/TRMM_3B42_Daily_7/summary, accessed on 5 December 2022).

(b) CHIRPS

Climate Hazards Group InfraRed Precipitation with Station data Version 2.0 (hereafter: CHIRPS) is based on infrared Cold Cloud Duration (CCD) observation [3]. Furthermore, this dataset is a composition of 0.05° climatology that includes satellite estimates, daily 0.05° CCD-based rainfall estimates, and gauge precipitation from weather stations. More information about the underlying algorithms used in CHIRPS can be found in Funk et al. [3]. CHIRPS daily datasets used in this study come from the University of California, Santa Barbara Channel (https://data.chc.ucsb.edu/products/CHIRPS-2.0/, accessed on 5 December 2022).

(c) TAMSAT

Tropical Applications of Meteorology using Satellite data and ground-based observations (Version 3.0: hereafter TAMSAT) was developed by the University of Reading in 1977. The underlying algorithm used in TAMSAT includes rainfall estimates based on the time-lapse analysis of the cloud-top temperature distribution observed every 30 min [39] from the thermal infrared (TIR) [7,40]. In addition, quality-controlled rain-gauge data are also used for the calibration of the TAMSAT estimates. The Version 3.0 used in this study is more accurate compared to Version 2.0; this is because Version 3.0 was based on a 5-day (pentad) time-step compared to a 10-day pentad in Version 2.0 [40]. Also, Version 3.0 better captured the local variabilities in rainfall climate [2].

(d) GPM IMERG

The GPM (IMERG, V06) satellite-based rainfall products include three products. The IMERG-Early Run (hereafter: IMERG-ER) is the GPM Level 3; this is an early dataset derived from the daily accumulation of the half-hourly version of the GPM (GPM_3IMERGHHE) [8]. This version of the IMERG is the earliest version and has around 4 h observation time and uses only forward propagation (morphing). The IMERG-Late Run (hereafter: IMERG-LR) product is also GPM Level 3; it is a late daily dataset derived from the daily accumulation of the half-hourly version of the GPM (GPM_3IMERGHHL) [8]. IMERG-LR consists of both forward and backward propagation (morphing). This version uses a climatological adjustment that includes gauge data [41]. IMERG-Final Run (hereafter: IMERG-FR) is the GPM Level 3 IMERG Final (GPM_3IMERGDF), which is also derived from the daily accumulation (24 h) of the half-hourly GPM_3IMERGHH. The dataset has a latency of ~3.5 months using forward, and backward propagation combined with monthly gauge analyses [8]. In other words, IMERG-FR is the only version with monthly gauge-observation adjustment when compared to other versions (IMERG-ER and IMERG-LR).

(3) Streamflow Data: African Database of Hydrometric Indices (ADHI)

According to Tramblay et al. [42], the ADHI is a hydrometric database consisting of "1466 stations with at least 10 years of daily discharge data over the period 1950–2018. The average record length is 33 years, and 131 stations have complete records over 50 years". These stations are spatially distributed across the entire African continent. For the UCRB, the stations inside this sub-basin are shown in Figure 1. As shown in Figure 2, only the stations "ADHI-49" and "ADHI-1391" have no missing values. In addition, the right panel (Figure 3) shows several types of missing patterns and their corresponding ratios. The missing and observed (present) values are represented by yellow and navy blue (Figure 2), respectively. Only these stations ("ADHI-49" and "ADHI-1391") without missing values will be used in the model calibration evaluation. As for the assessment performance evaluation of the satellite products, only "ADHI-1391" will be used. This is to avoid bias and misinterpretation if the stations with missing values are used. Furthermore, monthly discharge datasets from the stations were further accumulated into the season time scale as rainy (March, April, May, June, July, August, September, October, and November) or dry (December, January, and February).

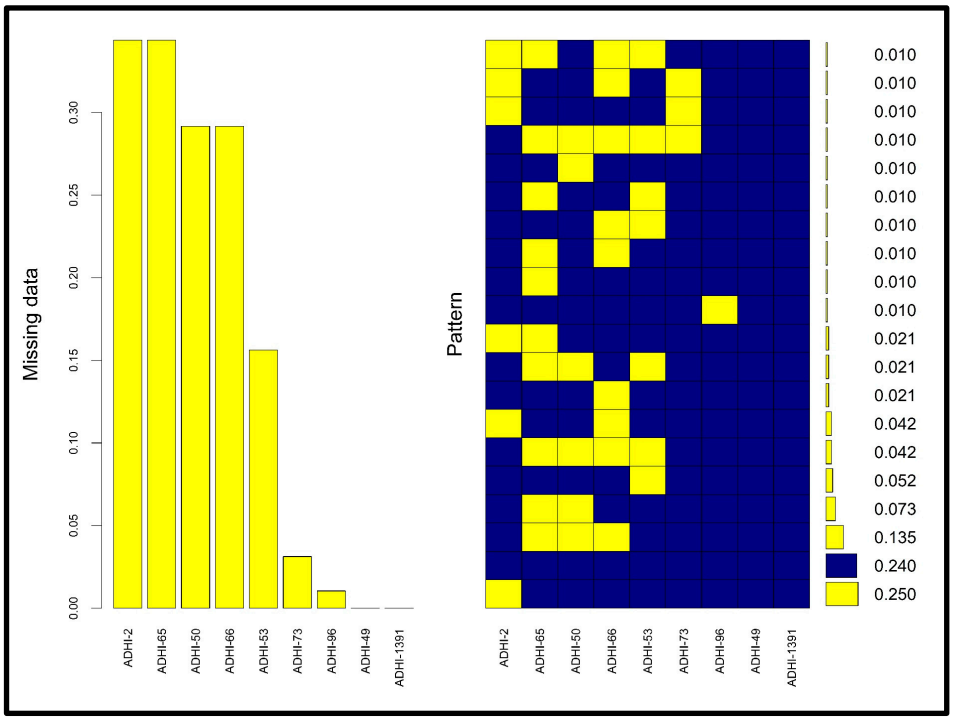

Figure 2. Visual representation of the missing monthly gauged discharge values from 1984–1991. The missing and observed (present) values are represented by yellow and navy blue, respectively (left panel: proportion of missingness, right panel: missingness pattern).

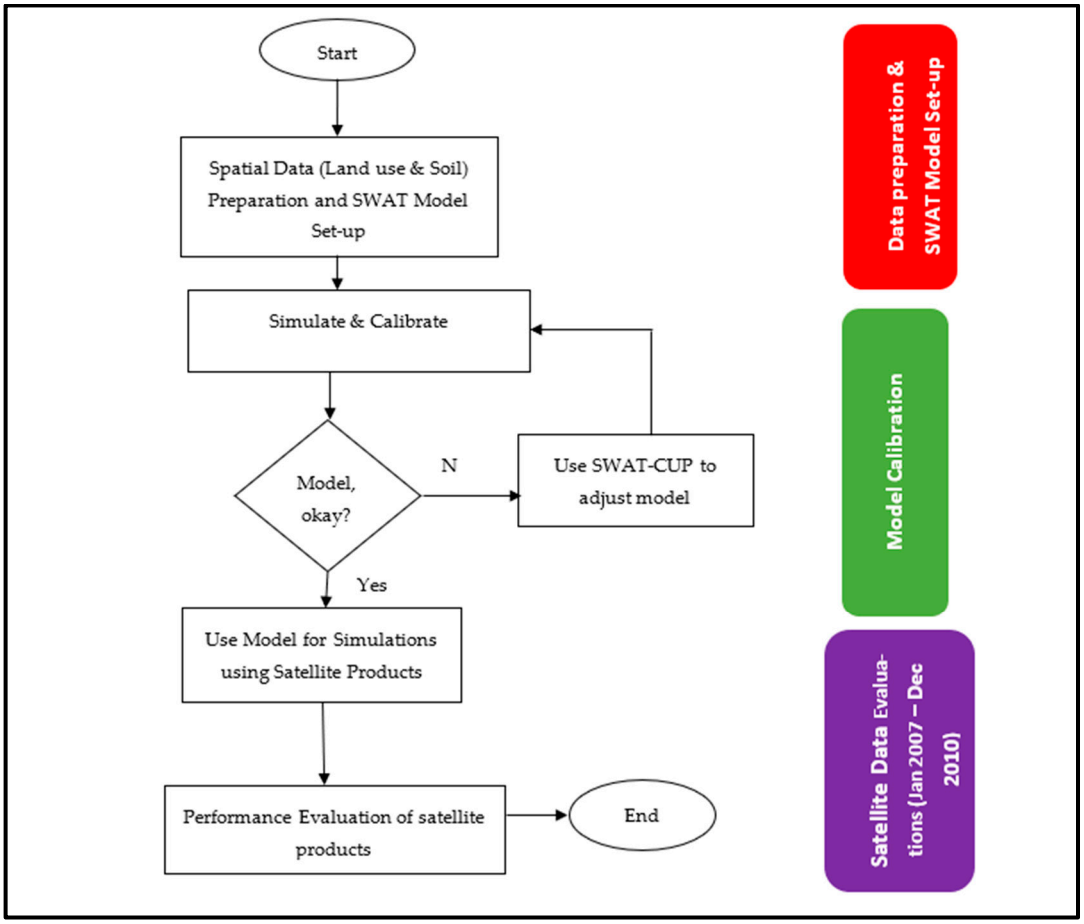

Figure 3. Flow chart of SWAT model development, calibration, validation, and evaluation of precipitation products for the Congo River Basin.

2.3. SWAT Model Hydrologic Processes and Set-Up

The SWAT model is semi-distributed [43] and based on the Curve Number (CN) method. The hydrologic process in SWAT is based on the hydrologic cycle, in which precipitation is the dominant process. SWAT can simulate both water quantity and quality. In other words, various agricultural management practices, such as the impacts of manure and fertilizer applications, as well as planting and harvesting dates, can be predicted. The concept of water balance (WB) is the key component of any hydrologic process. Using this concept, each component of the hydrologic cycle can be evaluated. In other words, WB provides the means to assess the relationship among all hydrologic processes, such as evapotranspiration (ET), surface flow (SF), and soil water content (SWC) due to plant development and water quality (i.e., pathogen, nutrient, and pesticide) fluxes. In the SWAT model, WB is defined as [44]:

$$SW_t = SW_o + \sum_{i=1}^{n} \left(R_{day} - Q_{surf} - E_a - w_{seep} - Q_{gw} \right) \quad (1)$$

where SW_t is the final water content (mm H_2O), SW_o is the antecedent soil water content, Q_{surf} is the accumulated runoff (mm H_2O), R_{day} is the rainfall depth (mm H_2O), E_a is the evapotranspiration (mm H_2O), w_{seep} is the water (mm H_2O) entering the vadose zone from the soil profile on the day i, and Q_{gw} is the return flow (mm H_2O).

The SWAT model simulates these processes in daily time steps. The model was developed to estimate the amount of runoff from a catchment under different soil and land use types [45,46].

$$Q_{surf} = \frac{\left(R_{day} - I_a\right)^2}{\left(R_{day} - I_a + S\right)} \quad (2)$$

Q_{surf} is the accumulated runoff (mm H_2O), R_{day} is the rainfall depth (mm H_2O), I_a is the initial abstractions prior to runoff (mm H_2O), and S is the retention parameter. Furthermore, the retention parameter can be simplified as:

$$S = 25.4\left(\frac{1000}{CN} - 10\right) \quad (3)$$

where CN is the Curve Number for the day, and Ia is usually defined as 0.2 S, making Equation (1):

$$Q_{surf} = \frac{(R_{day} - 0.2S)^2}{\left(R_{day} + 0.8S\right)} \quad (4)$$

In other words, runoff will take place whenever R_{day} is greater than I_a. A GIS platform is required to prepare all the spatial inputs needed in SWAT. A Hydrologic Response Unit (HRU) is created from the intersection of soil type, land use, and topographic features (i.e., slope). The HRU is the smallest computational unit used to simulate the hydrologic response in any basin. More information about runoff conceptualization in SWAT can be found in [44]. The sequential procedure used to set up the modeling and evaluation performed in this study are shown in Figure 3. The SWAT-CUP program developed by Abbasapour [47] was used for the sensitivity analysis and calibration of the model. This step is necessary to quantify the range of parameters to modify during the calibration process. This also helps in saving time and reducing computation costs for a large basin such as the UCRB. Table 1 shows the spatial and temporal resolutions of the satellite products used in this study.

Table 1. Climate data sources and spatial and temporal resolutions of datasets used in the evaluation.

Dataset Used	Period	Spatial and Temporal Resolution	Source
CHIRPS v2	2007–2010	0.05° × 0.05°, daily	University of California, Santa Barbara Channel (https://data.chc.ucsb.edu/products/CHIRPS-2.0/, accessed on 5 December 2022)
TAMSAT v3	2007–2010	0.0375° × 0.0375°, daily	TAMSAT Research Group Channel (https://www.tamsat.org.uk/data/archive, accessed on 5 December 2022)
TMPA	2007–2010	0.25° × 0.25, daily	Tropical Rainfall Measuring Mission (TRMM) (2011), TRMM (TMPA/3B43) Rainfall doi:10.5067/TRMM/TMPA/MONTH/7
IMERG (ER, LR, and FR)	2007–2010	0.1° × 0.1°, daily	GPM IMERG Final Precipitation L3 1 day 0.1 degree × 0.1 degree V06, Edited by Andrey Savtchenko, Greenbelt, MD, Goddard Earth Sciences Data and Information Services Center (GES DISC), Accessed: [5 December 2022], doi:10.5067/GPM/IMERGDF/DAY/06

3. Results

3.1. Spatial Variability of Satellite-Based Rainfall Products

Figure 4 shows the spatial distribution of the average annual rainfall for all the satellite products. The light blue color represents low values, while the dark blue color represents high values. In other words, the annual average precipitation values in the UCRB vary from approximately 1041 to more than 3000 mm. All products underestimated CFSR. There is a clear similarity between IMERG-ER and IMERG-LR, with high values and low values at the southern and northern portions of the plots, respectively. In addition, IMERG-FR and TMPA show similar patterns and spatial distributions across the map. This is evidence of their being integrated with gauged precipitation in their algorithms. CHIRPS also shows a similar pattern compared to these two products (TMPA & IMERG-FR). It would be interesting to see if these spatial patterns, variability, and similarities among all the products would propagate when used as hydrologic forcing through SWAT.

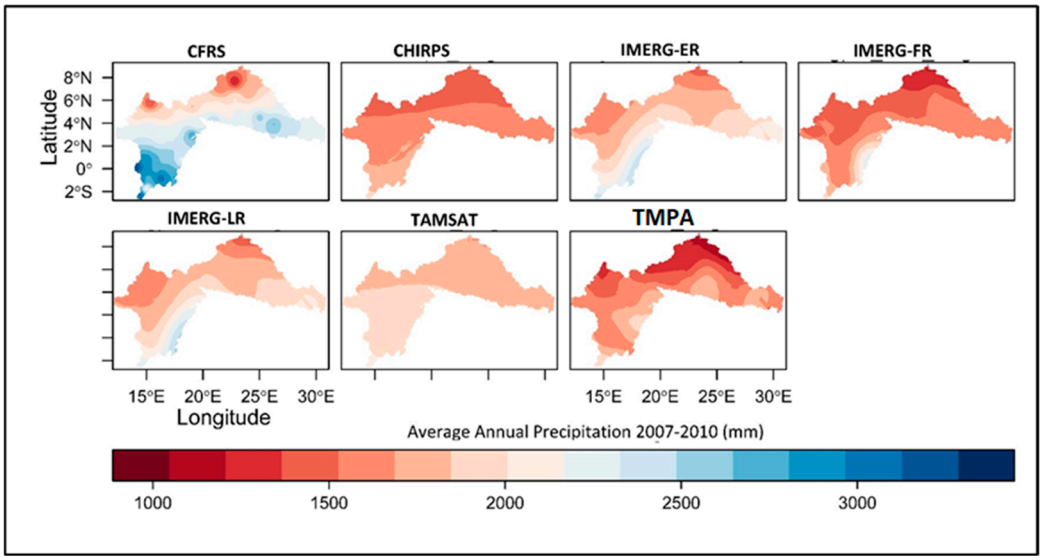

Figure 4. Spatial Distribution of Average Annual Precipitation (mm/yr.) for CFSR, TMPA, TAMSAT, CHIRPS, IMERG-ER, IMERG-LR, and IMERG-FR.

3.2. Descriptive Statistical Evaluation of Predicted Discharges

The Nash-Sutcliffe efficiency (NSE), percent bias (PBIAS), Kling–Gupta efficiency (KGE), and the ratio of the root mean square error to the standard deviation of measured data (RSR) for the CFSR-calibrated model (Gauge #: ADHI_1391) are 0.4, 2.9, 0.7, and 0.78, respectively (see Supplementary Materials). Similarly, NSE, PBIAS, KGE, and RSR for the CFSR-calibrated model (Gauge #: ADHI_49) are 0.4, 6, 0.7, and 0.79, respectively. Although NSE above 0.5 is recommended as satisfactory by Moriasi et al. [48], Motovilov et al. [49] also suggested an adequate value within the range of 0.36–0.75. KGE is 0.7 at both hydrometric stations; a value above 0.5 is considered satisfactory. Furthermore, PBIAS for ADHI_1391 and ADHI_49 is 2.9 and 6, respectively. Both values are within the ±25 suggested as acceptable by Moriasi et al. [48]. The similarities in the performance metrics for these two hydrometric stations are expected since they are on the same trunk of the Ubangi River and approximately 78 km apart. Furthermore, the hydrography plot (ADHI_1391: see Supplementary Materials) shows that the CFSR-calibrated model responded and captured the rising and descending limbs. Although there is evidence of overestimation in the earlier part of the time series, the calibration satisfactorily captured the seasonality of the hydrology. Notably, the gauged discharge used in this calibration is the average value of measured flow; therefore, the simulated values may still be within range. With this performance, this calibrated model can be used as the benchmark for all the hydrologic forcings using satellite products. The satellite product evaluation will be

performed only at ADHI_1391. The objective of the CFSR-calibrated model is to provide an even playing field for all the satellite products when used as hydrologic forcing.

The descriptive statistics of the discharge of each satellite product and how they compared with OBSERVED are shown in Table 2. The average discharge by CHIRPS, TAMSAT, and TMPA is 3036.9 m^3/s, 2538.3 m^3/s, 4929.7 m^3/s, and 3595.6 m^3/s, respectively. It is clear that TAMSAT overestimated the average OBSERVED discharge (2994.6 m^3/s). For the IMERG products, both IMERG-ER (5592.9 m^3/s) and IMERG-LR (5592.9 m^3/s) overestimated the OBSERVED, whereas IMERG-FR (3312.4 m^3/s) seems closer to the OBSERVED. This further confirms that IMERG-FR already has gauged precipitation integrated. In terms of low flow (minimum discharge), CHIRPS, TAMSAT, and TMPA have a minimum flow of 227 m^3/s, 197.0 m^3/s, and 862 m^3/s, respectively. Thus, TMPA overpredicted the minimum flow when compared with the OBSERVED (371 m^3/s). For the IMERG products, IMERG-ER, IMERG-LR, and IMERG-FR have a minimum flow of 230.0 m^3/s, 334.0 m^3/s, and 234.0 m^3/s, respectively. Only IMERG-LR is closer to the OBSERVED. For the maximum flow, all the satellite products overestimated the OBSERVED. This shows that care must be taken when using these datasets for extreme event (e.g., flooding) prediction, especially for use in block maxima analysis, such as Generalized Extreme Value Distribution.

Table 2. Descriptive statistics of the rainfall satellite estimation as hydrologic forcing in the Congo River Basin.

Statistics	OBSERVED	CHIRPS	TAMSAT	TMPA	IMERG-ER	IMERGE-LR	IMERG-FR
Mean (m^3/s)	2994.6	3036.9	4929.7	3595.6	4588.9	5592.9	3312.4
Standard Deviation (m^3/s)	2418.5	3122.4	4715.7	2661.1	4697.7	4515.0	3001.3
Coefficient of Variation (%)	80.8	102.8	95.7	74.0	102.4	80.7	90.6
Skewness	0.8	1.0	0.8	1.1	1.3	1.1	1.2
Minimum (m^3/s)	371.4	227.0	246.0	862.0	230.0	334.0	234.0
Maximum (m^3/s)	7976.0	10,300	16,300	10,100	17,300	18,700	12,200

Figure 5 shows the correlation matrix plot of the monthly discharge between OBSERVED and CHIRPS, TAMSAT, TMPA, and all the IMERG products from 2007 to 2010. The estimates from CHIRPS and TMPA were correlated with OBSERVED with a value of $r = 0.95$ and 0.93, respectively. This is an indication of good linear relationships with gauged discharge in UCRB. Furthermore, IMERG-ER, IMERG-LR, and IMERG-FR have a correlation of 0.89, 0.91, and 0.95 with OBSERVED, respectively. This is also evidence of a strong linear relationship. For TAMSAT, the correlation value was 0.96. Indeed, TAMSAT has the highest correlation value of all the satellite products; however, using only linear relationship criteria to quantify the performance of a rainfall product may be misleading. There is a need to test if the rainfall product will capture peak flow and seasonality and reproduce the rising and receding of the limbs of the hydrograph. These properties are crucial in quantifying the hydrologic response of any river basin. In general, all the satellite products have a good linear relationship with measured discharge.

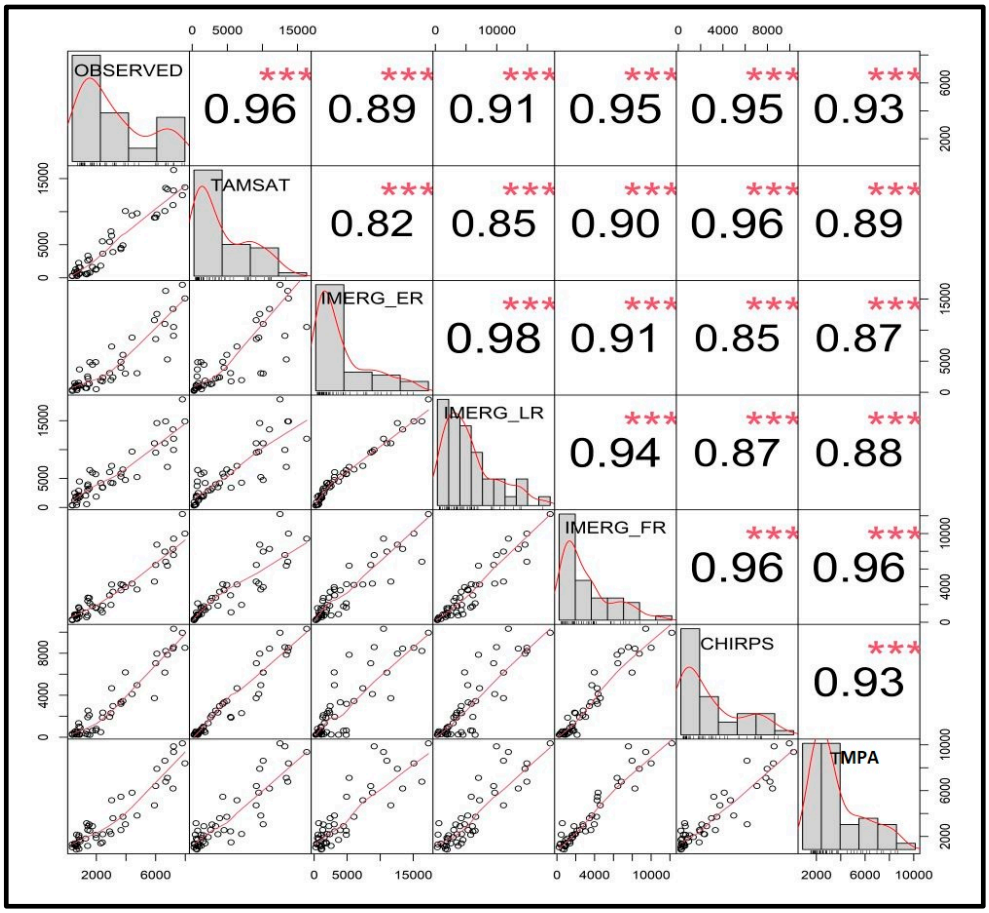

Figure 5. Scatterplot matrix showing the histograms, kernel density overlays, absolute correlation, and significance levels (*** $p < 0.001$) between OBSERVED, TMPA, CHIRPS, IMERG-FR, IMERG-LR, IMERG-ER, and TAMSAT monthly discharge estimates for the years 2007–2010.

3.3. Monthly and Seasonal Evaluation of Monthly Discharge Using Satellite Products as Hydrologic Forcing

Figure 6a–f shows the hydrograph of the satellite products against the OBSERVED discharge from January 2007 to December 2010. TMPA and CHIRPS compared well with OBSERVED, as shown in Figure 6a,b. It is also interesting to see that both satellite products adequately reproduced the timing of rising and receding limbs of the hydrograph for all years. For high flow years (2007 and 2008), these two products slightly overestimated the peak discharge. During the low flow year (2009), TMPA performed better than CHIRPS. In general, these two products reproduced well the seasonality from year to year. This good agreement with OBSERVED further confirms the underlying algorithm of these two products (i.e., inclusion of gauge precipitation). In Figure 6c–e, all the IMERG overestimated the OBSERVED, except for IMERG-FR (Figure 6d). From year to year, IMERG-FR consistently agreed with OBSERVED from both timing and magnitude perspectives. This further shows the evidence of gauge precipitation already included in this product. The overestimation in IMERG-ER and IMERG-LR shows that they must be bias-corrected before being applied in hydrologic studies. The performance of these products (IMERG-ER and IMERG-LR) is also consistent with the patterns and similarities seen in previous sections. The hydrography of the year-to-year performance of TAMSAT is shown in Figure 6f. Both products overestimated the OBSERVED flow. The overestimating tendencies seen with these two products are consistent with the average annual spatial distribution pattern seen and discussed in Section 3.1. Figure 7a–c shows the seasonal Box-and-Whisker plots for 2007, 2008, 2009, and 2010. For these periods, there were variabilities from year to year, as shown in the 25th and 75th percentiles. The whisker (which is the range of the data) is

highest for TAMSAT, IMERG-LR, and IMERG-ER. These products exhibited wetness, as shown in their spatial distributions in Section 3.4. CHIRPS, TMPA, and IMERG-FR show similar patterns when compared with OBSERVED. These performances and behaviors are consistent with the similar patterns shown in previous sections.

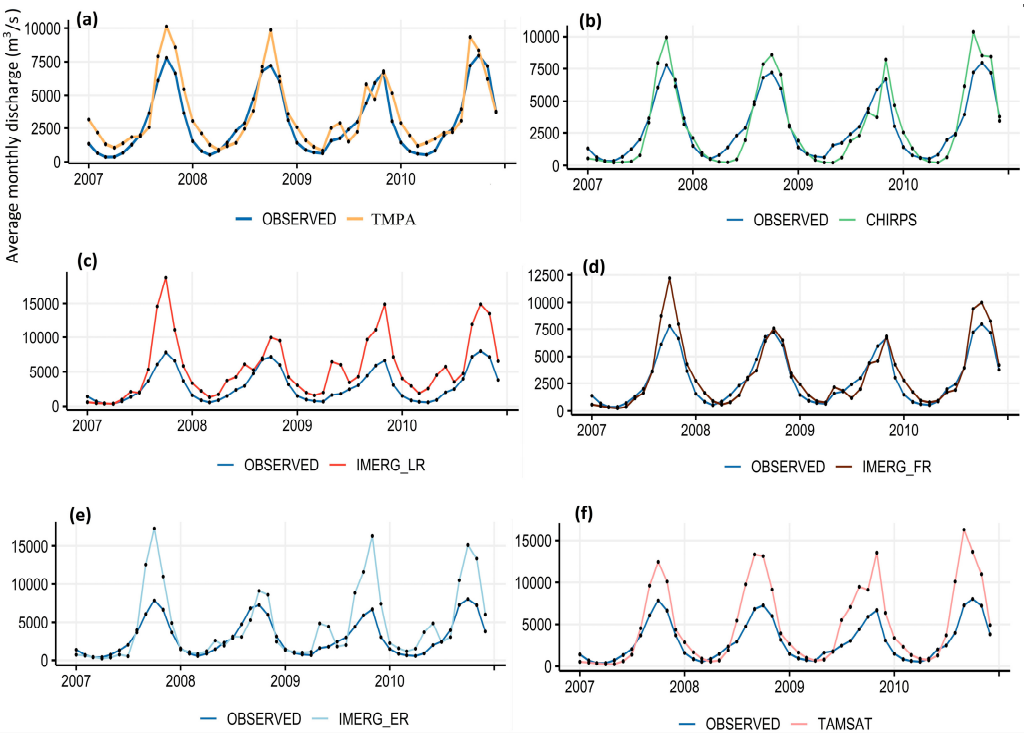

Figure 6. Monthly Discharge Plots from 2007–2010 for (**a**) TMPA, (**b**) CHIRPS, (**c**) IMERG-LR, (**d**) IMERG-FR, (**e**) IMEG_ER, and (**f**) TAMSAT.

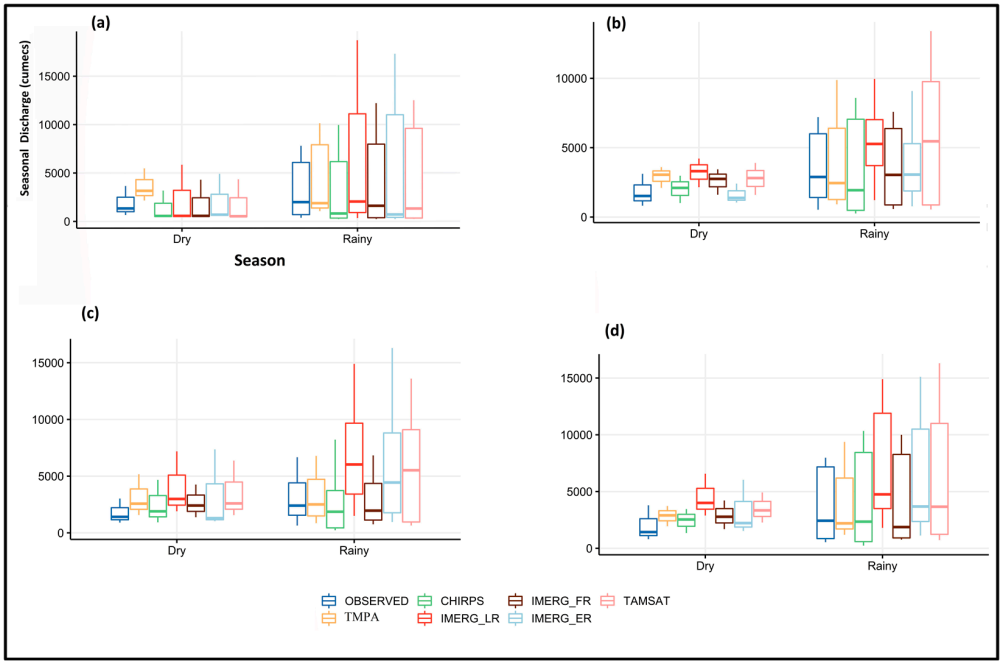

Figure 7. Box-and-Whisker Plot showing OBSERVED, CHIRPS, IMERG-FR, IMERG-ER, IMERG-LR, TMPA, and TAMSAT average monthly discharge estimates for the years (**a**) 2007, (**b**) 2008, (**c**) 2009, and (**d**) 2010.

Table 3 shows the performance of each satellite product based on the metrics introduced by [49]. The NSE for CHIRPS, IMERG-FR, and TMPA was 0.79, 0.80, and 0.77, respectively. These NSE values show that these satellite products are skillful in reproducing the gauged discharge. TAMSAT, IMERG-ER, and IMERG-LR have NSE values of −0.94, −0.73, and −1.26, respectively. This shows that the average OBSERVED is a better predictor than all aforementioned satellite products. The above performance is consistent with the performance discussed in previous sections. Similar trends of performance are also seen when KGE values are considered. For the PBIAS, CHIRPS and IMERG-FR have 1.4 and 10.6, respectively. This shows that they are closer to zero (optimal) when compared with other satellite products. RMSE values for CHIRPS, TMPA, and IMERG-FR are 1087 m^3/s, 1159 m^3/s, and 1081 m^3/s, respectively. In addition, TAMSAT, IMERG-ER, and IMERG-LR have RMSE values of 3334 m^3/s, 3148 m^3/s, 3169 m^3/s, and 3599 m^3/s, respectively. The RSR for CHIRPS, TMPA, and IMERG-FR is the same (0.45), whereas TAMSAT, IMERG-ER, and IMERG-LR have RSR values of 1.38, 1.3, 1.31, and 1.5, respectively. With the optimal value being zero, it is clear that CHIRPS, TMPA, and IMERG-FR outperformed all other products.

Table 3. Hydrologic model performance for satellite-based rainfall products and OBSERVED discharge using the SWAT model.

	CHIRPS	TMPA	TAMSAT	IMERG-ER	IMERG-LR	IMGERG-FR
NSE	0.79	0.77	−0.73	−0.75	−1.26	0.8
KGE	0.7	0.76	−0.149	−0.087	−0.229	0.731
PBIAS	1.4	20.1	64.6	53.2	86.8	10.6
RMSE	1087	1159	3148	3169	3599	1081
RSR	0.45	0.48	1.3	1.31	1.5	0.45

3.4. Performance Evaluation Using the Water Balance Components

Further evaluation of WB components was performed based on three key components of the hydrologic processes. For brevity purposes, the WB for the UCRB of the satellite products performed based on an average month from 2007–2010 are shown in Figure 8a–c. For the average surface runoff (Figure 8a, mm/month), this is the runoff contribution from the streamflow; CHIRPS has the lowest range throughout the year. Low flows during the dry months (DJF) and high flows during the wet months are clearly partitioned in the time series plot. It is interesting to see that IMERG-FR and TMPA show a similar pattern and variability throughout the year. TAMSAT has the highest runoff during the wet months. This pattern is consistent with TAMSAT's behavior seen in previous sections. The implication of this pattern is that overestimated precipitation values propagate through the hydrologic model, leading to high runoff prediction. Figure 8b shows the average AET (mm/month) for all the products. All the products have a similar pattern, with high values during the wet months and low values during the dry months. This pattern is expected since high plant activity (transpiration) and moisture vaporization (evaporation) will be high during the wet months and low during the dry months, when plant activities and moisture availability will be low. Notably, IMERG-ER and IMERG-LR have similar ranges, behaviors, and patterns for both seasons. SWC (Figure 8c, mm/month) is the average amount of water stored in the soil profile throughout the period of simulation. The monthly fluctuations of all the satellite products follow the expected behavior for a watershed in this region and are also synchronous with other components of the WB discussed above. In addition, it is expected that SWC should be correlated with seasonal precipitation patterns (i.e., high values in the wet months and low values in the dry months). It is also interesting to see that the IMERG products (IMERG-ER and IMERG-LR) without monthly gauge adjustment follow the same pattern.

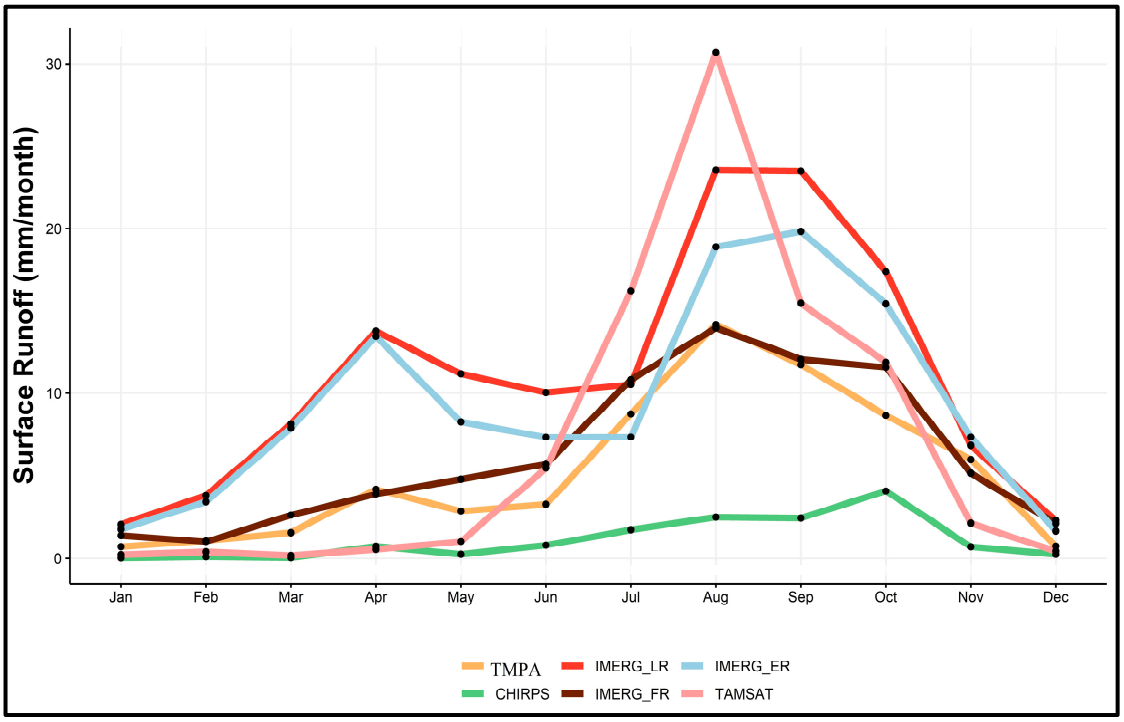

(**a**)

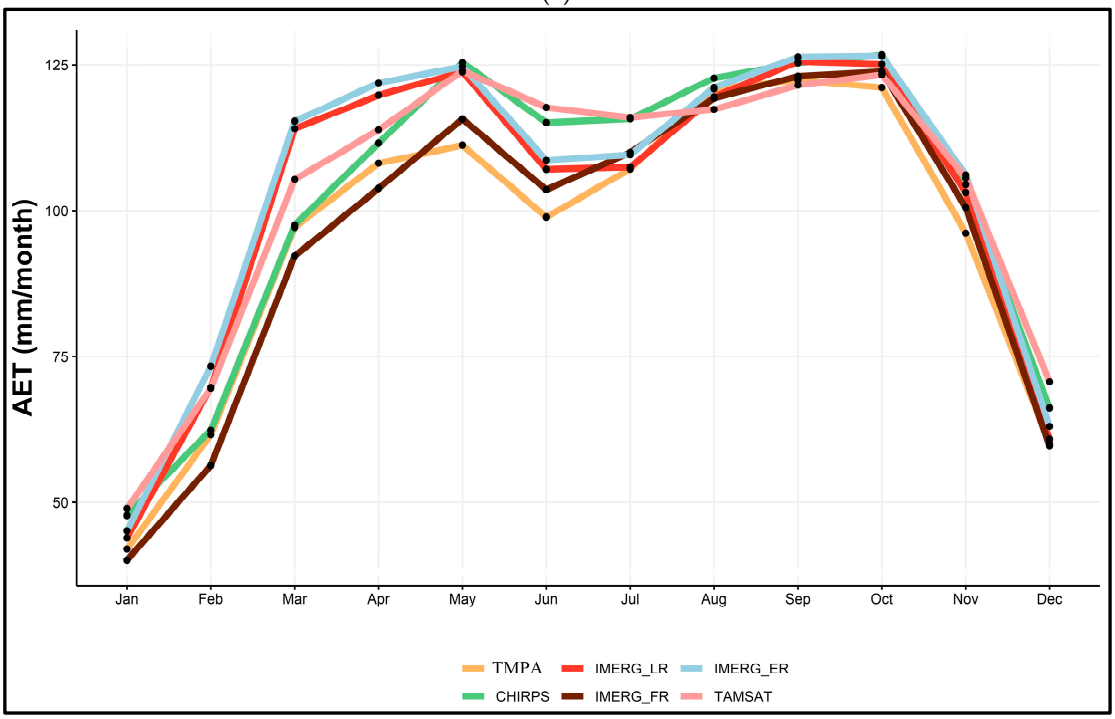

(**b**)

Figure 8. *Cont.*

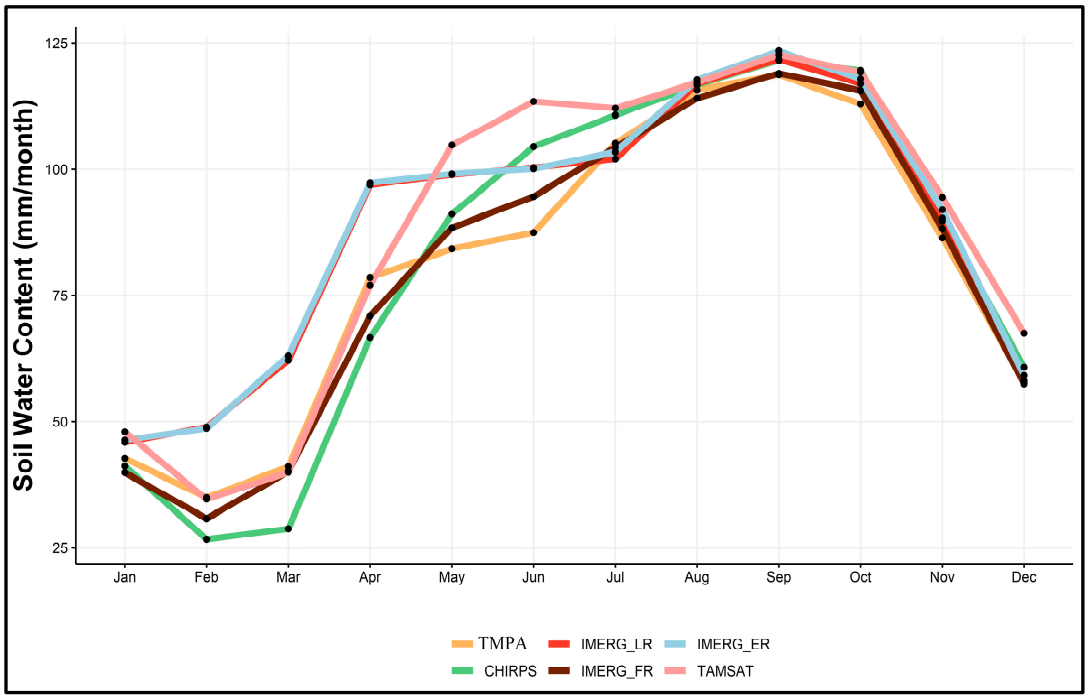

(**c**)

Figure 8. (**a**): Predicted Average Monthly Surface Runoff (mm/month) from 2007–2010 for the Upper Congo River Basin. (**b**): Predicted Average Monthly Actual Evapotranspiration (mm/month) from 2007–2010 for the Upper Congo River Basin. (**c**): Predicted Average Monthly Soil Water Content (mm/month) from 2007–2010 for the Upper Congo River Basin.

Finally, the close similarities between IMERG products and TMPA are due to the common underlying algorithm. TMPA is based on an active precipitation radar and passive microwave imager, while the IMERG products are based on a dual-frequency precipitation radar and advanced passive microwave sensors. Meanwhile, TAMSAT is based on infrared satellite data and calibrated with gauged precipitation. CHIRPS combines infrared data, gauged observation, and climatological datasets. This underlying algorithm plays a role in their performance, as seen in this study. IMERG products, with their varied latencies, provide added advantages in monitoring processes that have temporal responsiveness of less than 24 h, such as flash floods or hurricanes.

4. Conclusions

This study evaluated important satellite-based rainfall estimates as forcing in a semi-distributed large river basin in Africa. The pertinent research question answered by this paper is as follows: How good are these satellite products in reproducing the hydrologic processes of the world's second largest river basin? Satellite-based products are very useful in poorly gauged regions. CHIRPS, TAMSAT, TMPA, IMERG-ER, IMERG-LR, and IMERG-FR are freely available satellite products whose comparative analysis together has not been performed for a large river basin such as the CRB. These products were used to force a calibrated SWAT model for the upper region of the CRB. The following remarks can be drawn from this study:

(a) All the precipitation products responded and reproduced well the timing and seasonality of the gauged discharge at Bangui hydrometric outlets of the UCRB. This was consistent for all the years. The seasonality and timing of the hydrographs is very important in hydrologic applications, such as flood monitoring and early warning preparedness.

(b) IMERG-FR, TMPA, and CHIRPS captured the peak flows. This is expected, since these products have been bias-corrected using gauged precipitation. This also shows the

similarities in their underlying algorithms (gauge-precipitation-adjusted). In addition, the results show that these products can be used as proxies for gauged precipitation, especially in sparsely gauged basins such as the CRB.

(c) Using the performance ratings recommended for monthly time steps by Moriasi et al. (2007) [48], the performance of CHIRPS and IMERG-FR can be rated as very good. TMPA can be said to be good and satisfactory. Other satellite products, such as TAMSAT, IMERG-ER, and IMERG-LR, are classified as unsatisfactory and show that some adjustments may be necessary before they can be used for practical hydrologic applications in the UCRB.

This research is a call for data collection services in the CRB. This would benefit hydrologists, water resource managers, ecologists, and other decision-makers with interest in the basin. Since all organizations and agencies who have worked in the CRB have the same goals of forest preservation, ecosystem services, water resource management, etc., a central geospatial portal should be created to house all the various datasets available in the basin for effective water resource management strategies. Rather than perform a generic evaluation, this study went further by hosting the results on a dashboard available at the African River Basin Geoportal.

Supplementary Materials: The following supporting information can be downloaded at: https://www.mdpi.com/article/10.3390/rs16203868/s1, Figure S1: Monthly discharge (hydrograph) at ADHI-1391 flow station based on CFSR-based precipitation forcing (1984–1991). Table S1: Hydrological model performance for CFSR-Model. Table S2: Qualitative summary of the performance of satellite-based estimates in the Upper Congo Basin using hydrologic attributes.

Funding: This research received no external funding.

Data Availability Statement: Datasets for satellite-based rainfall are available at various portals such as CHIRPS (https://www.chc.ucsb.edu/data/chirps), TAMSAT (https://research.reading.ac.uk/tamsat/), TMPA (https://disc.gsfc.nasa.gov/datasets/TRMM_3B42_Daily_7/summary), IMERG (https://disc.gsfc.nasa.gov/datasets/GPM_3IMERGDE_06/summary) (accessed on 6 December 2022).

Acknowledgments: The author would like to thank two anonymous reviewers for their useful suggestions, which helped in improving the quality of this paper.

Conflicts of Interest: The author declares no conflicts of interest.

References

1. Fortin, V.; Roy, G.; Donaldson, N.; Mahidjiba, A. Assimilation of radar quantitative precipitation estimations in the Canadian Precipitation Analysis (CaPA). *J. Hydrol.* **2015**, *531*, 296–307. [CrossRef]
2. Boluwade, A. Remote Sensed-Based Rainfall Estimations over the East and West Africa Regions for Disaster Risk Management. *ISPRS J. Photogramm. Remote Sens.* **2020**, *167*, 305–320. [CrossRef]
3. Funk, C.; Peterson, P.; Landsfeld, M.; Pedreros, D.; Verdin, J.; Shukla, S.; Husak, G.; Rowland, J.; Harrison, L.; Hoell, A.; et al. The climate hazards infrared precipitation with stations—A new environmental record for monitoring extremes. *Sci. Data* **2015**, *2*, 150066. [CrossRef] [PubMed]
4. Huffman, G.J.; Bolvin, D.T.; Nelkin, E.J.; Wolff, D.B.; Adler, R.F.; Gu, G.; Hong, Y.; Bowman, K.P.; Stocker, E.F. The TRMM Multisatellite Precipitation Analysis (TMPA): Quasi-global, multiyear, combined-sensor precipitation estimates at fine scales. *J. Hydrometeorol.* **2007**, *8*, 38–55. [CrossRef]
5. Huffman, G.J.; Bolvin, D.T.; Nelkin, E.J.; Adler, R.F. *TRMM (TMPA) Precipitation L3 1 Day 0.25 Degree × 0.25 Degree V7*; Savtchenko, A., Ed.; Goddard Earth Sciences Data and Information Services Center (GES DISC): Greenbelt, MD, USA, 2017. Available online: https://disc.gsfc.nasa.gov/datasets/TRMM_3B42_Daily_7/summary (accessed on 5 December 2022). [CrossRef]
6. Huffman, G.J.; Stocker, E.F.; Bolvin, D.T.; Nelkin, E.J.; Tan, J. *GPM IMERG Final Precipitation L3 1 Month 0.1 Degree × 0.1 Degree V06*; Goddard Earth Sciences Data and Information Services Center (GES DISC): Greenbelt, MD, USA, 2023. Available online: https://disc.gsfc.nasa.gov/datasets/GPM_3IMERGM_07/summary (accessed on 22 January 2020). [CrossRef]
7. Maidment, R.I.; Grimes, D.; Black, E.; Tarnavsky, E.; Young, M.; Greatrex, H.; Allan, R.P.; Stein, T.; Nkonde, E.; Senkunda, S.; et al. A new, long-term daily satellite-based rainfall dataset for operational monitoring in Africa. *Nat. Sci. Data* **2017**, *4*, 170063. [CrossRef]
8. Huffman, G.J.; Bolvin, D.T.; Braithwaite, D.; Hsu, K.; Joyce, R.; Kidd, C.; Nelkin, E.J.; Sorooshian, S.; Tan, J.; Xie, P. *Algorithm Theoretical Basis Document (ATBD) Version 5.2 for the NASA Global Precipitation Measurement (GPM) Integrated Multi-Satellite Retrievals for GPM (I-MERG)*; GPM Project: Greenbelt, MD, USA, 2019; p. 38.

9. Ashouri, H.; Hsu, K.L.; Sorooshian, S.; Braithwaite, D.K.; Knapp, K.R.; Cecil, L.D.; Nelson, B.R.; Prat, O.P. PERSIANN-CDR: Daily precipitation climate data record from multisatellite observations for hydrological and climate studies. *Bull. Am. Meteorol. Soc.* **2015**, *96*, 69–83. [CrossRef]
10. Joyce, R.J.; Janowiak, J.E.; Arkin, P.A.; Xie, P. CMORPH: A Method that Produces Global Precipitation Estimates from Passive Microwave and Infrared Data at High Spatial and Temporal Resolution. *J. Hydrometeor.* **2004**, *5*, 487–503. [CrossRef]
11. Novella, N.S.; Thiaw, W.M. African Rainfall Climatology Version 2 for Famine Early Warning Systems. *J. Appl. Meteorol. Climatol.* **2013**, *52*, 588–606. [CrossRef]
12. Munzimi, Y.A.; Hansen, M.C.; Adusei, B.; Senay, G.B. Characterizing Congo Basin Rainfall and Climate Using Tropical Rainfall Measuring Mission (TRMM) Satellite Data and Limited Rain Gauge Ground Observations. *J. Appl. Meteorol. Climatol.* **2015**, *54*, 541–555. [CrossRef]
13. Nicholson, S.E.; Klotter, D.; Zhou, L.; Hua, W. Validation of Satellite Precipitation Estimates over the Congo Basin. *J. Hydrometeorol.* **2019**, *20*, 631–656. [CrossRef]
14. Camberlin, P.; Barraud, G.; Bigot, S.; Dewitte, O.; Makanzu Imwangana, F.; Maki Mateso, J.-C.; Martiny, N.; Monsieurs, E.; Moron, V.; Pellarin, T.; et al. Evaluation of remotely sensed rainfall products over Central Africa. *Q. J. R. Meteorol. Soc.* **2019**, *145*, 2115–2138. [CrossRef]
15. Becker, M.; Papa, F.; Frappart, F.; Alsdorf, D.; Calmant, S.; da Silva, J.S.; Prigent, C.; Seyler, F. Satellite-based estimates of surface water dynamics in the Congo River Basin. *Int. J. Appl. Earth Obs. Geoinf.* **2018**, *66*, 196–209. [CrossRef]
16. Becker, M.; Da Silva, J.S.; Calmant, S.; Robinet, V.; Linguet, L.; Seyler, F. Water Level Fluctuations in the Congo Basin Derived from ENVISAT Satellite Altimetry. *Remote Sens.* **2014**, *6*, 9340–9358. [CrossRef]
17. Crowley, J.W.; Mitrovica, J.X.; Bailey, R.C.; Tamisiea, M.E.; Davis, J.L. Land water storage within the Congo Basin inferred from GRACE satellite gravity data. *Geophys. Res. Lett.* **2006**, *33*, L19402. [CrossRef]
18. Datok, P.; Fabre, C.; Sauvage, S.; N'kaya, G.D.M.; Paris, A.; Santos, V.D.; Laraque, A.; Sánchez-Pérez, J.-M. Investigating the Role of the Cuvette Centrale in the Hydrology of the Congo River Basin. In *Congo Basin Hydrology, Climate, and Biogeochemistry*; Tshimanga, R.M., N'kaya, G.D.M., Alsdorf, D., Eds.; John Wiley & Sons: Hoboken, NJ, USA, 2022. [CrossRef]
19. Kitambo, B.; Papa, F.; Paris, A.; Tshimanga, R.M.; Calmant, S.; Fleischmann, A.S.; Frappart, F.; Becker, M.; Tourian, M.J.; Prigent, C.; et al. A combined use of in situ and satellite-derived observations to characterize surface hydrology and its variability in the Congo River basin. *Hydrol. Earth Syst. Sci.* **2022**, *26*, 1857–1882. [CrossRef]
20. World Bank. Journey into the Congo Basin—The Lungs of Africa and Beating Heart of the World. 2022. Available online: https://www.worldbank.org/en/news/feature/2022/10/24/journey-into-the-congo-basin-the-lungs-of-africa-and-beating-heart-of-the-world (accessed on 19 December 2023).
21. WWF. Congo Basin Facts. Available online: https://www.worldwildlife.org/places/congo-basin (accessed on 1 June 2023).
22. Laraque, A.; Moukandi N'kaya, G.D.; Orange, D.; Tshimanga, R.; Tshitenge, J.M.; Mahé, G.; Nguimalet, C.R.; Trigg, M.A.; Yepez, S.; Gulemvuga, G. Recent Budget of Hydroclimatology and Hydrosedimentology of the Congo River in Central Africa. *Water* **2020**, *12*, 2613. [CrossRef]
23. Arnold, J.G.; Williams, J.R.; Nicks, A.D.; Sammons, N.B. *SWRRB: A Basin Scale Simulation Model for Soil and Water Resources Management*; Texas A & M University Press: College Station, TX, USA, 1990; p. 142.
24. Schuol, J.; Abbaspour, K.C.; Yang, H.; Srinivasan, R.; Zehnder, A.J. Modeling blue and green water availability in Africa. *Water Resour. Res.* **2008**, *44*, W07406. [CrossRef]
25. Tomy, T.; Sumam, K.S. Determining the Adequacy of CFSR Data for Rainfall-Runoff Modeling Using SWAT. *Procedia Technol.* **2016**, *24*, 309–316. [CrossRef]
26. Minh Tuan, B.; Lu, J.; Nie, L. Evaluation of the Climate Forecast System Reanalysis data for hydrological model in the Arctic watershed Målselv. *J. Water Clim. Chang.* **2021**, *12*, 3481–3504. [CrossRef]
27. Tshimanga, R.M. Two Decades of Hydrologic Modeling and Predictions in the Congo River Basin. In *Congo Basin Hydrology, Climate, and Biogeochemistry*; Tshimanga, R.M., N'kaya, G.D.M., Alsdorf, D., Eds.; John Wiley & Sons: Hoboken, NJ, USA, 2022. [CrossRef]
28. Lambert, T.; Bouillon, S.; Darchambeau, F.; Massicotte, P.; Borges, A.V. Shift in the chemical composition of dissolved organic matter in the Congo River network. *Biogeosciences* **2016**, *13*, 5405–5420. [CrossRef]
29. Mushi, C.A.; Ndomba, P.M.; Trigg, M.A.; Tshimanga, R.M.; Mtalo, F. Assessment of basin-scale soil erosion within the Congo River Basin: A review. *CATENA* **2019**, *178*, 64–76. [CrossRef]
30. Tshimanga, R.M. Hydrological Uncertainty Analysis and Scenario-Based Stream Flow Modelling for the Congo River Basin. Ph.D. Thesis, Rhodes University Repository, Grahamstown, South Africa, 2012.
31. Runge, J. Of deserts and forests: Insights into Central African palaeoenvironments since the Last Glacial Maximum. *Palaeoecol. Afr.* **2008**, *28*, 15–27.
32. Laraque, A.; Mahé, G.; Orange, D.; Marieu, B. Spatiotemporal variations in hydrological regimes within Central Africa during the XXth century. *J. Hydrol.* **2001**, *245*, 104–117. [CrossRef]
33. Aloysius, N.; Saiers, J. Simulated hydrologic response to projected changes in precipitation and temperature in the Congo River basin. *Hydrol. Earth Syst. Sci.* **2017**, *21*, 4115–4130. [CrossRef]
34. Alsdorf, D.; Beighley, E.; Laraque, A.; Lee, H.; Tshimanga, R.; O'Loughlin, F.; Mahé, G.; Dinga, B.; Moukandi, G.; Spencer, R.G.M. Opportunities for hydrologic research in the Congo Basin. *Rev. Geophys.* **2016**, *54*, 378–409. [CrossRef]

35. Nguimalet, C.R.; Orange, D. Caractérisation de la baisse hydrologique actuelle de la rivière Oubangui à Bangui, République Centrafricaine. *La Houille Blanche* **2019**, *105*, 78–84. [CrossRef]
36. Dile, Y.T.; Srinivasan, R. Evaluation of CFSR climate data for hydrologic prediction in data-scarce watersheds: An application in the Blue Nile River Basin. *J. Am. Water Resour. Assoc. (JAWRA)* **2014**, *50*, 1226–1241. [CrossRef]
37. Fuka, D.R.; MacAllister, C.A.; Degaetano, A.T.; Easton, Z.M. Using the Climate Forecast System Reanalysis dataset to improve weather input data for watershed models. *Hydrol. Proc.* **2013**, *28*, 5613–5623. [CrossRef]
38. Huffman, G.J.; Bolvin, D.T.; Braithwaite, D.; Hsu, K.; Joyce, R.; Kidd, C.; Nelkin, E.J.; Xie, P. *NASA Global Precipitation Measurement (GPM) Integrated Multi-Satellite Retrievals for GPM (IMERG). Algorithm Theoretical Basis Document (ATBD) Version, 4*; NASA: Washington, DC, USA, 2018.
39. Universität Hamburg. Rainfall Estimates for Africa from TAMSAT. Available online: https://www.cen.uni-hamburg.de/en/icdc/data/atmosphere/tamsat-rainfall-africa.html (accessed on 1 June 2023).
40. Maidment, R.I.; Grimes, D.; Allan, R.P.; Tarnavsky, E.; Stringer, M.; Hewison, T.; Roebeling, R.; Black, E. The 30-year TAMSAT African Rainfall Climatology And Time series (TARCAT) data set. *J. Geophys. Res.* **2014**, *119*, 10619–10644. [CrossRef]
41. NASA's Integrated Multi-Satellite Retrievals for GPM (IMERG). Available online: https://gpm.nasa.gov/data/imerg (accessed on 1 June 2023).
42. Tramblay, Y.; Rouché, N.; Paturel, J.E.; Mahé, G.; Boyer, J.F.; Amoussou, E.; Bodian, A.; Dacosta, H.; Dakhlaoui, H.; Dezetter, A.; et al. ADHI: The African database of hydrometric indices (1950–2018). *Earth Syst. Sci. Data* **2021**, *13*, 1547–1560. [CrossRef]
43. Arnold, J.G.; Srinivasan, R.; Muttiah, R.S.; Williams, J.R. Large area hydrologic modeling and assessment part I: Model development. *JAWRA J. Am. Water Resour. Assoc.* **1998**, *34*, 73–89. [CrossRef]
44. Neitsch, S.L.; Arnold, J.G.; Kiniry, J.R.; Williams, J.R. *Soil and Water Assessment Tool Theoretical Documentation Version 2009*; Texas Water Resources Institute: College Station, TX, USA, 2011.
45. SWAT. Chapter 32: SWAT Output Data: Primary Output Files. 2005. Available online: https://swat.tamu.edu/media/69395/ch32_output.pdf (accessed on 4 December 2022).
46. Rallison, R.E.; Miller, N. Past, present and future SCS runoff procedure. In *Rainfallrunoff Relationship—Proceedings of the International Symposium on Rainfall-Runoff Modelling*; Singh, V.P., Ed.; Water Resources Publications: Littleton, CO, USA, 1981.
47. Abbaspour, C.K. SWAT-CUP SWAT Calibration and Uncertainty Programs. 2012. Available online: https://swat.tamu.edu/media/114860/usermanual_swatcup.pdf (accessed on 10 January 2023).
48. Moriasi, D.N.; Arnold, J.G.; Van Liew, M.W.; Bingner, R.L.; Harmel, R.D.; Veith, T.L. Model evaluation guidelines for systematic quantification of accuracy in watershed simulations. *Trans. ASABE* **2007**, *50*, 885–900. [CrossRef]
49. Motovilov, Y.G.; Gottschalk, L.; Engeland, K.; Rodhe, A. Validation of a distributed hydrological model against spatial observations. *Agric. For. Meteorol.* **1999**, *98*, 257–277. [CrossRef]